

# Contribution of the MR spectroscopic imaging in the diagnosis of prostate cancer in the peripheral zone

Emanuele Casciani,<sup>1</sup> Elisabetta Poletti,<sup>1</sup> Luca Bertini,<sup>1</sup> Gabriele Masselli,<sup>1</sup>  
Paolo Emiliozzi,<sup>2</sup> Mostafà Amini,<sup>2</sup> Vito Pansadoro,<sup>3</sup> Gian Franco Gualdi<sup>1</sup>

<sup>1</sup>Department of Radiology, University of Rome “La Sapienza”, Via del Policlinico, 155, 00166 Rome, Italy

<sup>2</sup>Department of Urology (EP) and Pathology (MA), S. Giovanni Addolorata Hospital, Rome, Italy

<sup>3</sup>Foundation Vincenzo Pansadoro, Rome, Italy

## Abstract

**Purpose:** To establish the additional value of 3D magnetic resonance spectroscopy (3D-MRS) imaging to endorectal MR imaging in the diagnosis of prostate cancer in the peripheral zone.

**Materials and methods:** MR imaging and MRS imaging were performed in 79 patients with suspicion of prostate cancer on the basis of digital rectal exploration, transrectal ultrasound and PSA level. All the examinations were performed with 1.5 T MR scan using an endorectal coil (transverse and coronal FSE T2-weighted sequences, axial SE T1-weighted and PRESS 3D CSI). MR examinations have been evaluated by two Radiologists blind of the clinical data in a “per patients” analysis. MR imaging and MRS imaging findings were compared with the result of histological data from radical prostatectomy in 53 patients and biopsy in 17 patients.

**Results:** Nine patients (11.4%) were excluded because of serious artefacts in the MR spectrum. The reported values of sensitivity, specificity, PPV and NPV for MR imaging alone were respectively 84%, 50%, 76% and 63% (LR+ 1.7; LR– 0.3). Instead the reported values of sensitivity, specificity, PPV and NPV for the combination of MR imaging to MRS imaging were respectively 89%, 79%, 89% and 79% (LR+ 4.28; LR– 0.14). We found an incremental benefit of MRS imaging to MR imaging for tumour diagnosis although these results did not show statistically significant differences.

**Conclusions:** The MRS imaging improves the accuracy of the endorectal MR imaging in the diagnosis of prostate cancer.

**Key words:** Magnetic resonance (MR) spectroscopy—Magnetic resonance (MR) diagnosis—Prostate—Neoplasm

High-resolution endorectal–pelvic-phased array MR imaging has demonstrated good sensitivity (78%–91%), but low specificity (27%–55%) in identifying tumour location because of a large number of false positives [1–5]. The diagnosis is based on the finding of low signal intensity on T2-weighted sequences, which is not specific and can also be detected with post-biopsy haemorrhage, prostatitis and sequelae resulting from radiation or hormonal treatment [1–3, 5, 6]. The recent introduction of 3D MR spectroscopy imaging (3D-MRSI) into clinical practice adds information to the morphological data of endorectal MR imaging, enabling a more specific diagnosis of prostate cancer. A number of in vitro [9–11] and in vivo studies [7, 8, 12–19] has found high choline levels and low citrate levels in the areas affected by prostate carcinoma. The results achieved so far with 3D-MRSI in prostate cancer identification [12], extracapsular extension [13], tumour volume [16], tumour aggressiveness [17], and changes produced by radiotherapy [18] or by hormone therapy [19] are promising, but the number of studies is still inadequate to prove its value. Furthermore, due to the fact that all the studies published to date have been conducted by a limited number of research groups, there is the need to demon-

strate the reproducibility of the results. The aim of this study is to define the contribution of 3D-MRSI to endorectal MR imaging in diagnosing prostate cancer in the peripheral zone in our institution.

## Materials and methods

### *Study population*

In this retrospective study we reviewed the endorectal MR imaging and 3D-MRSI prostate scans of 79 patients who presented to us with suspected prostate cancer based on digital rectal exploration (DRE) and/or on transrectal ultrasound (TRUS) and/or PSA levels. The minimum inclusion criteria were an increment in prostate consistency at DRE, a visible nodule in the peripheral zone at TRUS or a PSA level greater than 4 ng/mL. For the inclusion, in the study, it was sufficient for patients to fulfill at least one of these criteria. All patients gave written informed consent and the study was approved by the local ethic committee. Average patient age was 68.1 years ( $\pm 5.2$ ). The mean PSA level at diagnosis was 9.54 ng/mL (range 4.5–40.4 ng/mL). All patients underwent biopsy after MRI (average interval 5 days; range 3–12 days). Fifty-three patients underwent laparoscopic radical prostatectomy. Patients with negative biopsy underwent a second biopsy 4–8 months later. None of the patients received preoperative hormonal or radiation therapy.

### *MR technique*

MR imaging was performed by using a 1.5-T whole-body MR imaging unit (Signa; GE Medical Systems, Milwaukee, Wis). The endorectal coil (Medrad, Pittsburgh, PA, USA) was connected to the pelvic phased-array coil, and combined images were obtained. The endorectal coil was positioned with the patient in a lateral recumbent position and 100 mL of room air was insufflated, after intravenous administration of 20 mg of butylscopolamine (Buscopan, Boehringer Ingelheim, Deutschland) to reduce intrinsic rectal movements and discomfort during examination. T2-weighted FSE sequences with the Driver Equilibrium Fast Recovery technique was performed in the transverse and coronal planes from the seminal vesicles to the prostatic apex, using the following parameters: TR/TE 4000–5000 ms/102 ms; ETL 15–17; 3-mm thick sections without interval; 14-cm field-of-view, 3 signals acquired, matrix 256  $\times$  192. Transverse T1-weighted SE sequence from the aortic bifurcation to the prostate to assess pelvic adenopathy (TR/TE 500–700 ms/12 ms, 5-mm thick sections, 1-mm gap, 2 signals acquired, 26-cm field-of-view, 512  $\times$  224 matrix, no phase wrap) were also obtained.

### *MR spectroscopy protocol*

For the 3D-MRS imaging, a PRESS 3D CSI (Point Resolved Spectroscopy 3D Chemical Shift Imaging) was

used. Selective spectral 180° re-focusing pulses were used to reduce the contaminating signals of water and lipids, respectively to the left of the choline peak and to the right of the lipid peak in the scale of frequencies. About 1024 signal encodings were performed, respectively 16  $\times$  8  $\times$  8 in *x*, *y* and *z*, for a total of 17 min of acquisition (TR 1000 ms). Acquisition FOV was 110-mm, with a spatial resolution of 0.24–0.70 cm<sup>3</sup>. The PRESS 3D CSI sequence was localised on the axial T2 images to obtain coverage of most of the prostate without the periprostatic fat. About 10–12 presaturation bands were also positioned to minimise contamination of the spectra by periprostatic fat.

### *MR images interpretation*

The MR scans were assessed by two radiologists, expert in prostate MR imaging (over 1000 examinations in the last 5 years), blinded to the clinical data, ultrasound findings, PSA levels and histological results. The quality of MR images was graded by using a three-point scale: one for diagnostic images; two for diagnostic images with few artefacts; three for non-diagnostic images with numerous artefacts.

Peripheral prostate signal alteration detected with MR imaging was graded on the basis of likelihood of tumour presence by using the following five-point scale: (a) certainly normal (high T2-signal intensity); (b) probably normal (linear or triangular hypointense alterations); (c) dubious (diffuse peripheral hypointensity, rounded or plaque-like hypointensities alterations); (d) probably pathological (rounded or plaque-like hypointensities with signs of minimal ECE); (e) certainly pathological (rounded or plaque-like hypointensities with signs of massive ECE). To simplify statistical calculations it was applied a dichotomy of the results considering scores of 1 and 2 as not-cancerous (negative) and scores of 3, 4 and 5 as cancerous (positive). Every patient was in this way registered as having not-cancerous lesions (lesions with a score of 1 or 2) or having one or more cancerous lesions (score of 3, 4 and 5).

### *Analysis of combined MR images and 3D-MRS imaging (MRI/3D-MRSI)*

The data of the PRESS 3D CSI sequence were automatically analysed by the 3D PROSE software both in the time domain—by means of a 2 Hz Lorentzian filter (apodization filter)—to reduce the spectral noise and improve their identification, and in the frequency domain—by means of phase correction (first point phasing correction). Subsequently, the spectra obtained were analysed by the Functool 2 software (General Electric, USA) with an algorithm for reconstruction and visualisation of the parametric images of the concentration of metabolites in the prostate. This software also allows

superimposition of the spectroscopic images on the axial anatomical imaging data. The metabolites choline, creatine and citrate were analysed considering their concentration within their respective areas. For each metabolite, the area under the peak was placed near the average value of signal intensities in the frequency interval of the corresponding metabolite, since the software was not used with the appropriate automatic integration function. Spectral evaluation was then carried out by using the axial T2 MR image as a reference. The spectral quality of each examination was subjectively rated as valuable or not valuable on the basis of signal-to-noise considerations, magnetic field homogeneity, overall shim and the presence of baseline distortions induced with water and lipid. Spectral quality was considered valuable if the signal-to-noise ratio of all metabolites was above eight; all metabolic resonances were reasonably well resolved, or there were minimal baseline distortions owing to residual water or lipid. Examinations with lower signal-to-noise ratios were considered of fair spectral quality, provided there was no lipid contamination. Examinations with substantial lipid contamination were considered to have poor spectral quality. Examinations with lower signal-to-noise ratios, with substantial lipid contamination or when peripheral zone coverage did not match with alterations found at MR imaging were considered to be not valuable.

The 3D-MRSI analysis was conducted to evaluate choline + creatine/citrate ((Cho + Cr)/Cit) ratio and the choline-to-creatine (Cho/Cr) ratio on the alterations revealed at MR exam.

The likelihood of the presence of prostate cancer was graded with a two-point scale: (a) normal (negative): (Cho + Cr)/Cit ratio < 0.75 and Cho/Cr ratio less than two SD (no decrease in polyamines); (b) abnormal (positive): hypointensities with a (Cho + Cr)/Cit ratio greater than two SD as compared to the normal population, i.e., >0.75, elevated choline, reduced or normal citrate with respect to background noise and Cho/Cr greater than two SD (decrease in polyamines).

### *Histopathological review*

All patients underwent biopsy after MRI (average interval 5 days; range 3–12 days). Two biopsies were taken for each side (right and left) and level (apex, middle portion and base), for a total of 12 biopsies per patient. Fifty-three patients, in which the biopsy revealed tumour cells, underwent radical prostatectomy through laparoscopy. The excised prostate was coloured on its surface with Indian ink and fixed in formalin. The paraffin-embedded, haematoxylin–eosin-stained histological sections were sliced at 3-mm intervals from the prostate base to apex in a plane perpendicular to the longitudinal axis of the gland, which was divided into right and left

lobe on three levels: apex (A), middle portion (M) and base (B). In all cases, the histological examination considered the presence or absence of findings compatible with prostate adenocarcinoma and the cell differentiation assessed according to the Gleason score.

The results of histopathological examination were then compared to MR imaging and MR spectroscopic findings and the results were registered on a “per patient” basis.

The comparison with the anatomical and pathological results was possible only in the cases in which both the morphological images and the MR spectrum were assessable.

### *Statistical analysis*

The statistical analysis was carried out by calculating sensitivity and specificity, positive and negative predictive values with CI 95%. We considered the likelihood ratio, particularly the positive; this value has an enormous practical value and it is becoming the preferred way of expressing and comparing the usefulness of different tests. Data were analyzed with Pearson Chi Square and McNemar test when appropriate.

## **Results**

The quality of morphological examinations (MR imaging) was diagnostic in all patients. The quality of MRSI was diagnostic without artefacts (score 1) in 45 patients (57%), diagnostic with few artefacts (score 2) in 25 patients (31.6%) and non-diagnostic with numerous artefacts (score 3) in 9 patients (11.4%).

Only in the 70 cases in which the spectrum proved to be diagnostic, it was possible to determine the contribution of the MRS imaging to the MR imaging alone. In 46 of 70 patients, the results of MR imaging and MRS imaging were compared with the histological results of radical prostatectomy and in 24 of 70 patients with results of needle biopsy. The histological examination revealed adenocarcinoma in 46 patients, prostatitis in 5 (aspecific  $n = 3$ ; tuberculous  $n = 2$ ) and no alterations in the remaining 19 patients.

The MR assessment based on the morphological scale described above yielded the following scores: lesions with a maximum score of 1 in 5 patients, 2 in 14 cases, 3 in 29 cases (Fig. 1), 4 in 13 cases and 5 in 9 cases (Fig. 2). In the identification of tumour in the peripheral zone of the prostate with MR imaging alone, the following values were obtained: sensitivity 84%, specificity 50%, PPV 76% and NPV 63%, with 12 false positives (Fig. 3) and 7 false negatives (Fig. 4).

The MRI/3D-MRSI evaluation, according to the two level scale described above, gave the following scores: 1 in 26 cases and 2 in 44 cases. In the identification of cancer in the peripheral portion of the prostate by MRI/

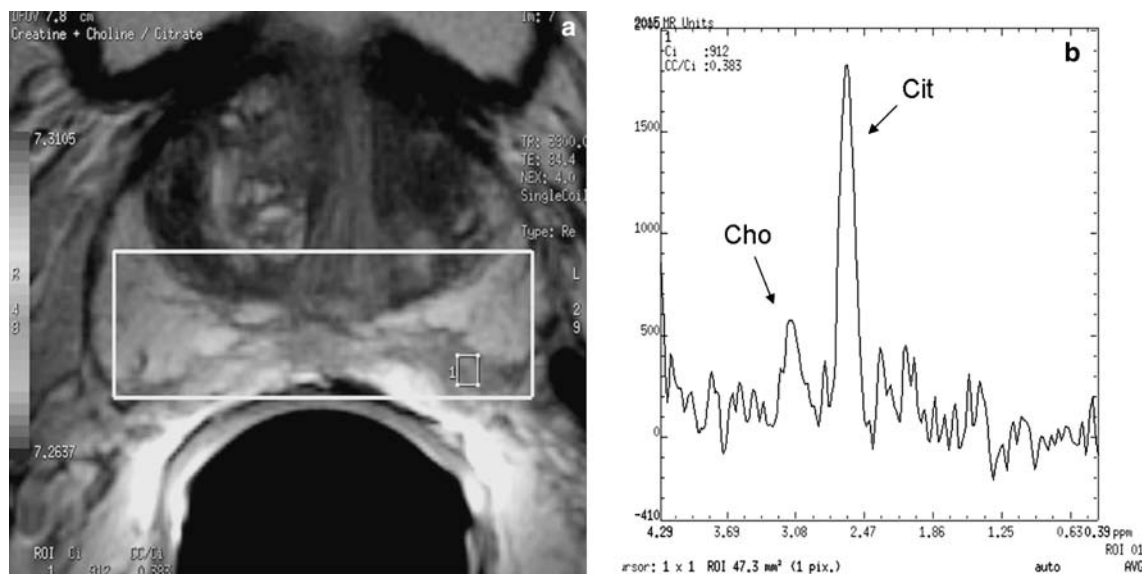


**Fig. 1.** FSE T2-weighted transverse MR image through the middle gland obtained with endorectal coil (**A**) and MR spectrum in the left peripheral zone (**B**). Area of decreased signal

intensity (MR score: 3) in the left peripheral zone (**A**) with normal spectrum pattern (citrate dominant and no abnormal elevation in choline) (**B**). Findings were confirmed by histopathology.

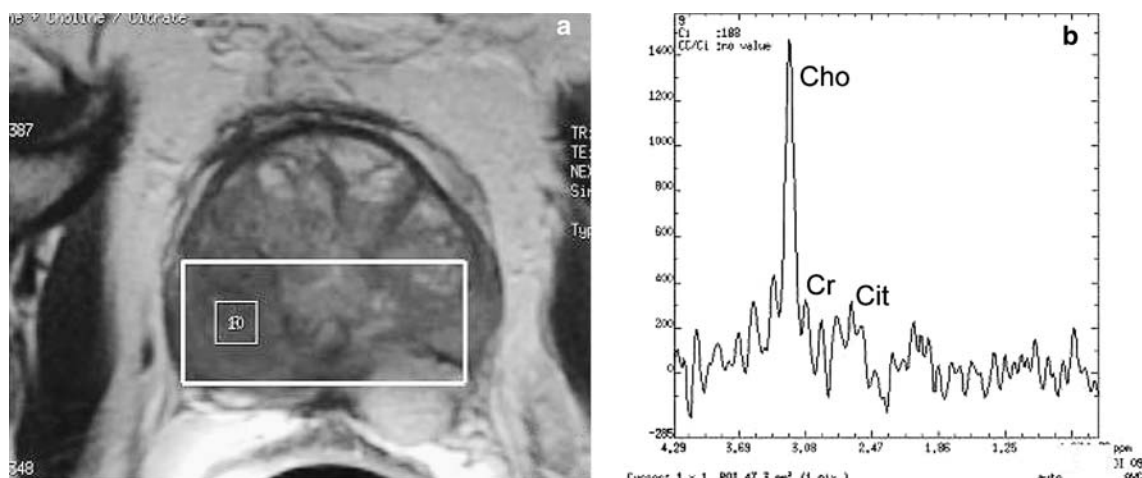


**Fig. 2.** FSE T2-weighted transverse MR image through the middle gland obtained with endorectal coil (**A**) and MR spectrum in the right peripheral zone (**B**). A tumor nodule is seen as an area of decreased signal intensity (MR score: 5) in the right peripheral zone with capsular penetration (**A**); at the

same level MR spectrum demonstrated elevated choline and reduced citrate and polyamines, a pattern consistent with high grade cancer (**B**). Findings were confirmed by histopathology high grade (Gleason 9) prostate cancer.

3D-MRSI, the following values were obtained: sensitivity 89%, specificity 79%, PPV 89% and NPV 79%, with five false positives and five false negatives. The positive likelihood ratio were, respectively, 1.70 (1.12–2.58) for MRI and 4.28 (1.25–9.39) for MRI/3D-MRSI and the negative likelihood ratio were, respectively, 0.30 (0.14–0.67) for MRI and 0.14 (0.06–0.32) for MRI/3D-MRSI (Table 1). The statistical relevance of these results were analyzed with the McNemar test but it did not show significant differences between the accuracy values of the two methods ( $P = 0.227$ ).

In all the patients with negative biopsy, the second biopsy resulted negative, too.

## Discussion

Although good results have been obtained on the contribution of MRS imaging to MR imaging in the identification of prostate cancer, the number of studies published so far is still limited. However, considering that most of the studies published up to now have been carried out by a limited number of research

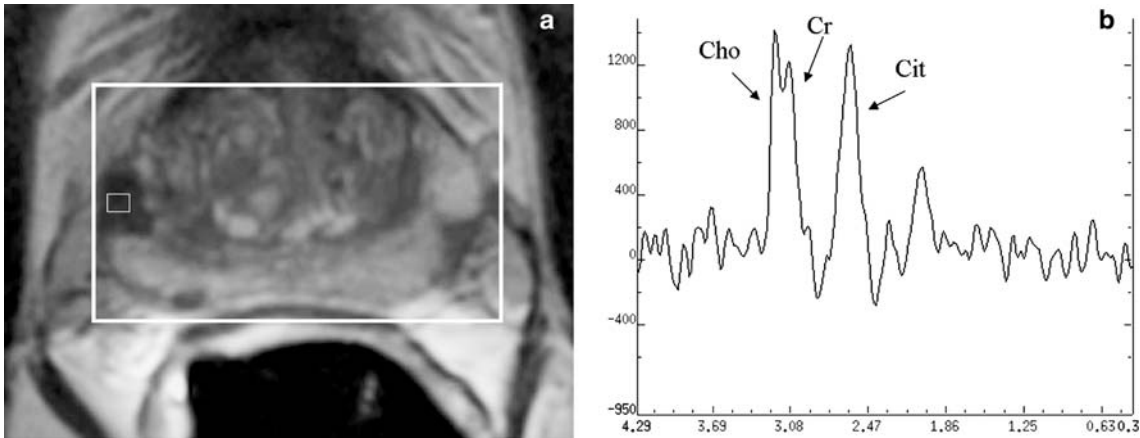


**Fig. 3.** Transverse T2-weighted fast spin-echo MR image (**A**) shows a focal area with well defined margins of decreased signal intensity in the peripheral zone of the right gland. MR spectrum obtained from the same area of imaging abnor-

mality in the right peripheral zone (**B**) demonstrates moderate elevated choline and normal citrate, a pattern consistent with low grade cancer. Histopathology from US-guided biopsy demonstrates granulomatous prostatitis.

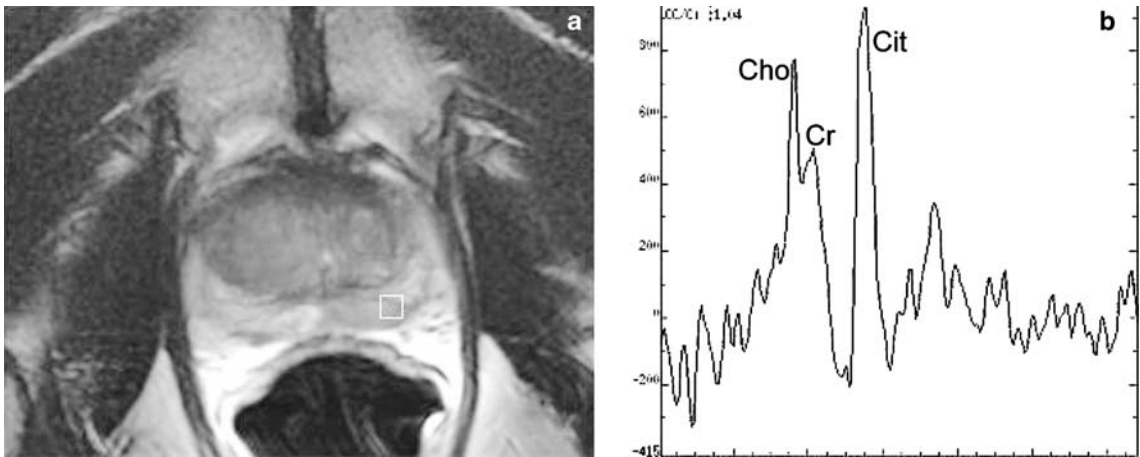


**Fig. 4.** Transverse T2-weighted fast spin-echo MR image through the middle gland (**A**) shows focal area of decreased signal intensity (MR score: 3) in the left peripheral zone. MR spectrum obtained from the same area (**B**) demonstrates

elevated choline and normal citrate, a pattern consistent with low grade cancer. Findings were confirmed by histopathology low grade (Gleason 5) prostate cancer

groups, there are limited chances to compare experiences to demonstrate the reproducibility of the data obtained.

The positive likelihood ratio has an enormous practical value and it is becoming the preferred way of expressing and comparing the usefulness of different tests. In our 70 patients the MRI/3D-MRSI has increased the odds of that diagnosis by a factor of 4.28 (CI 95% 1.95–9.39) respect to MR imaging alone.

In the 70 cases by MRI/3D-MRSI, the sensitivity, specificity and accuracy in the identification of peripheral prostate cancer showed an improvement, respect to MR imaging alone; the data obtained were sensitivity 89% and specificity 79% with MRI/3D-MRSI, against a sensitivity of 84% and a specificity of 50% with MR imaging alone. Our results are in line with that of other authors

[12, 20] which also registered increasing of the specificity (87%) MRI/3D-MRSI respect to MR imaging alone (79%).

The five false negatives we obtained are presumably to be referred to the dimensions (diameter less than 9 mm) as well as to the low Gleason score ( $3 + 3 = 6$ ) of the tumours, which were neither identified through the morphological exam, nor through the MRS imaging, in relation to the spatial resolution of the methodology. A region containing a small focus of cancer with a high (Cho + Cr)/Cit might be partially diluted by the presence of normal tissue within the same spectroscopic voxel, creating a false-negative reading.

In the five false positives in which the peripheral zone of the prostate appeared diffusely low signal intensity on the T2-weighted sequence and the MRS imaging showed

**Table 1.** Sensitivity, specificity, PPV, NPV, LRP and LRN of MRI and MR-MRSI

Tests	MRI		MRI-MRSI	
	Value (%)	95% CI	Value (%)	95% CI
Sensitivity	84	0.72–0.92	89	0.77–0.95
Specificity	50	0.31–0.69	79	0.60–0.91
Positive predictive value	76	0.63–0.86	89	0.77–0.95
Negative predictive value	63	0.41–0.81	79	0.60–0.91
Likelihood ratio positive	1.70	1.12–2.58	4.28	1.95–9.39
Likelihood ratio negative	0.30	0.14–0.67	0.14	0.06–0.32

an increased concentration of choline, the biopsy demonstrated prostatitis. In recent studies [21, 22] choline was elevated with histopathologically confirmed chronic prostatitis, with a metabolic pattern mimicking the one of cancer, with consequent false-positive findings.

We believe it is important to focus the attention on some potential technical limits of the software actually available. First, the time required to acquire high-quality spectroscopy images is still too long. Second, only a limited volume of the prostate could be imaged, and a portion of either the base or apex is excluded in patients with large glands. In our study, MRS imaging could not add any diagnostic information to MR imaging because of artefacts that obscured the metabolic frequency range in nine patients (11.4%). Even in the Jung et al. study [20], a significant number of patients (15/37) with poor or fair spectral data were excluded. In our study, the artefacts have been determined in five cases by the patient's movement (body motion and peristaltic movements) presumably due to the length of the sequence. In spite of the use of drug for smooth muscle relaxation, and the accurate instruction to the patient to be motionless, these five patients were not able to be motionless for 17 min (the spectroscopic sequence time is not changeable). In other two patients, we registered periprostatic fat tissue artefacts due to the very large and irregularity shape glands. In the last two patients we registered urine artefacts in patients who had previously undergone transurethral resection of the prostate, because of an open bladder neck. When the spectroscopic volume is set with the software at our disposal, it is necessary a compromise between the volume which can be studied and the spectrum quality. If an attempt is made to include the whole of the peripheral portion, it is easier to find artefacts in the contamination spectrum with the periprostatic tissues. On the other hand, if the volume to be explored is smaller, the spectrum quality improves, but the more peripheral regions could be excluded from the spectroscopic evaluation. However, even in the studies by Scheilder et al. [12] and Yu et al. [13] the coverage of the peripheral portion has been, respectively, less than 50% in 18/53 and 20/53 patients and only 12 of them have obtained coverage of the peripheral portion between 75% and 100%.

This study has an important limitations. As with prior studies [8, 16, 17] concerning the investigation of MR imaging and MRS imaging in prostate cancer, we only included tumours in the peripheral zone, because heterogeneity in the hyperplastic transition zone of older men limits tumour depiction.

The results obtained in this study, together with those published by the few groups that have investigated prostate MRS imaging, demonstrate the potential clinical utility of the metabolic information.

In conclusion, in spite of the improvements achieved so far, further technological developments are desirable, in order to reduce the time necessary to examine a spectroscopic sequence, to improve the anatomic coverage of the spectroscopic volume as well as to identify new metabolic markers with specific tissue type, markers for cellular proliferation, apoptosis and neoangiogenesis, considering that there is overlapping between tumour and inflammatory tissues.

## References

1. Presti JC, Hricak H, Narayan PA, et al. (1996) Local staging of prostatic carcinoma: comparison of transrectal sonography and endorectal MR imaging. *AJR* 166:103–108
2. Jager GJ, Ruijter ET, Van de Kaa CA, et al. (1996) Local staging of prostate cancer with endorectal MR imaging: correlation with histopathology. *AJR* 166:845–852
3. Hricak H, White S, Vigneron D, et al. (1994) Carcinoma of the prostate gland: MR imaging with pelvic phased-array coils versus integrated endorectal–pelvic phased-array coils. *Radiology* 193:703–709
4. Schiebler M, Schnall MD, Pollack HM, et al. (1993) Current role of MR imaging in the staging of adenocarcinoma of the prostate. *Radiology* 189:339–352
5. White S, Hricak H, Forstner R, et al. (1995) Prostate cancer: effect of postbiopsy haemorrhage on interpretation of MR images. *Radiology* 195:385–390
6. Quint LE, Van Erp JS, Bland PH, et al. (1991) Carcinoma of the prostate: MR images obtained with body coils do not accurately reflect tumour volume. *AJR* 156:511–516
7. Casciani E, Gualdi GF (2006) Prostate cancer: value of magnetic resonance spectroscopy 3D chemical shift imaging. *Abdom Imaging* (online first)
8. Kurhanewicz J, Vigneron DB, Hricak H, et al. (1996) Three-dimensional H-1 MR spectroscopic imaging of the in situ human prostate with high (0.24–0.7-cm<sup>3</sup>) spatial resolution. *Radiology* 198:795–805
9. Yacoe ME, Sommer G, Peehl D (1991) In vitro proton spectroscopy of normal and abnormal prostate. *Magn Reson Med* 19:429–438
10. Cornel EB, Heerschap A, Smits GA, et al. (1994) Magnetic resonance spectroscopy detects metabolic differences between seven

- Dunning rat prostate tumour sublines with different biological behaviour. *Prostate* 25:19–28
11. Cornel EB, Smits GA, Oosterhof GO, et al. (1993) Characterization of human prostate cancer, benign prostatic hyperplasia and normal prostate by in vitro <sup>1</sup>H and <sup>31</sup>P magnetic resonance spectroscopy. *J Urol* 150:2019–24
  12. Scheidler J, Hricak H, Vigneron DB, et al. (1999) Prostate cancer: localization with three-dimensional proton MR spectroscopic imaging—clinicopathologic study. *Radiology* 213:473–480
  13. Yu K, Scheidler J, Hricak H, et al. (1999) Prostate cancer: prediction of extracapsular extension with endorectal MR imaging and three-dimensional proton MR spectroscopic imaging. *Radiology* 213:481–488
  14. Vilanova JC, Barcelò J (2005) Prostate cancer detection: MR spectroscopic imaging. *Abdom Imag* (online first)
  15. Aboagye EO, Bhujwala ZM (1999) Malignant transformation alters membrane choline phospholipid metabolism of human mammary epithelial cells. *Cancer Res* 59:80–84
  16. Coakley FV, Kurhanewicz J, Lu Y, et al. (2002) Prostate cancer tumour volume: measurement with endorectal MR and MR spectroscopic imaging. *Radiology* 223:91–97
  17. Kurhanewicz J, Vigneron DB, Males RG, et al. (2000) The prostate: MR imaging and spectroscopy—present and future. *Radiol Clin North Am* 38:115–138
  18. Amsellem-Ouazana D, Younes P, Conquya S, et al. (2005) Negative prostatic biopsies in patients with a high risk of prostate cancer: is the combination of endorectal MRI and magnetic resonance spectroscopy imaging (MRSI) a useful tool? A preliminary study. *Eur Urol* 47:582–586
  19. Mueller-Lisse UG, Swanson MG, Vigneron DB, et al. (2001) Hormone ablation of localized prostate cancer: time-dependent therapy effects on prostate metabolism detected by 3D <sup>1</sup>H MR spectroscopy. *Magn Reson Med* 46:49–57
  20. Jung JA, Coakley FV, Vigneron DB, et al. (2004) Prostate depiction at endorectal MR spectroscopic imaging: investigation of a standardized evaluation system. *Radiology* 233:701–708
  21. Shukla-Dave A, Hricak H, Eberhardt S, et al. (2004) Chronic prostatitis: MR imaging and <sup>1</sup>H MR spectroscopic imaging findings—initial observations. *Radiology* 231:717–724
  22. Casciani E, Poletini E, Bertini L, et al. (2005) Granulomatous prostatitis: a pitfall in endorectal MR imaging and 3D MR spectroscopic imaging. *Eur J Radiol Extra* 54:111–114